Variable Flip Angle Schedules for Detecting Prepared Longitudinal Magnetization in Snapshot Balanced SSFP

T. B. Smith[1], Z. Zun[1], E. Wong[2], and K. S. Nayak[1]

[1]Department of Electrical Engineering, University of Southern California, Los Angeles, CA, United States, [2]Departments of Radiology and Psychiatry, University of California, San Diego, La Jolla, CA, United States

Introduction: Tissue characterization by MRI often involves the subtraction of images obtained with and without a preparation of the longitudinal magnetization (e.g. T_2 preparation, arterial spin labeling, and diffusion preparation). Studies based on snapshot balanced steady state free precession (SSFP) typically hasten the approach to the steady state by using a brief catalyzation [1] and constant flip angle during acquisition [2,3]. Operating in the transient state, however, provides an opportunity to improve performance. We introduce variable flip angle schedules optimized for the detection of differences in the prepared magnetization for a specific tissue of interest.

Methods: We developed a Bloch equation simulator to model the differential magnetization behavior when subjected to an arbitrary sequence of flip angles. The model subtracts the detected signals from two transient SSFP acquisitions (one with and one without preparation), each having identical TR, bandwidth, and resolution. Using this model, we ran a sequential quadratic programming algorithm to find flip angle schedules that optimized various functions of the detected difference signals for both a deionized water phantom (to measure our model's fidelity) and for myocardial tissue (to compare with constant-angle performance in vivo). We incorporated effects from off resonance and RF inhomogeneity [4] by simulating and averaging signals across 2/3 of the SSFP bandwidth (1/TR) and over appropriate B_1 scale factors. All schedules used 96 repetitions with TR = 3.2 ms, and the maximum angle was constrained to 70º. To reduce the complexity of searching this high-dimensional space, we ran a sequence of optimizations with progressively larger dimensionalities (while maintaining a constant total acquisition time) to seed the subsequent optimization routines (Fig. 1). We found this method had favorable acceleration and convergence behavior. We made three schedules for the phantom (T_1 = T_2 = 1300 ms): one to maximize the SNR, one to minimize the k-space apodization (ie, "flatten" the difference signal), and one to maximize the minimum value of the difference signal (Fig. 2). Using no assumptions about the tissue's k-space profile, we defined maximum SNR as the maximum average gain across all repetitions. Using these phantom schedules, we acquired the zero phase encode line every repetition in order to compare the simulated and measured difference signal profiles. For myocardium (T_1 = 1100 ms, T_2 = 40 ms [5]), we generated the variable-angle schedule that maximized SNR and the best constant-angle schedule for SNR (Fig. 2). For the myocardium scans, we acquired complete 2DFT data from three healthy volunteers using cardiac gating and linear view ordering. Our pulse sequence consisted of two snapshot acquisition intervals, each utilizing the same flip angle schedule, separated by a non-selective saturation pulse. We performed all collections on a GE Signa 3T EXCITE HD system.

Results and Discussion: The strong agreement between our simulation and the measured difference signals for the phantom is depicted in Figure 3. This agreement demonstrates that our model accurately simulates the differential magnetization behavior when exposed to an arbitrary sequence of flip angles, and is thus a well-founded basis for customizing schedules to effect a desired response. Figure 4 displays the difference images from the constant- and variable-angle schedules designed for maximum myocardial SNR. Compared with the best constant-angle schedule, our variable flip angle schedule improved the myocardial SNR in the three volunteers by an average of 18% (the minimum improvement was 14%) without adding image artifacts. We believe it is possible to improve these SNR results further by incorporating the tissue's k-space profile into the optimization or by tailoring the view ordering. Also, it is worth noting that this optimization technique is applicable to standard, non-subtractive SSFP applications as well.

Conclusion: The proposed approach finds the transient SSFP flip angle schedule that optimizes any objective metric (eg, maximum SNR) of the detected signal acquired from a differentially prepared magnetization scheme. The technique is compatible with any type of longitudinal magnetization preparation, and only requires knowledge of the TR length and tissue relaxation times. In myocardial tissue, this technique produced an 18% average SNR improvement over the conventional approach without introducing artifacts in the difference images.

References: [1] Nishimura, et al. ISMRM 2000: 301. [2] Scheffler, et al. Eur. Radiology 2003; 13: 2409-18. [3] Martirosian, et al. MRM 2004; 51: 353-361. [4] Sung, et al. JMRI 2008; 27: 643-48. [5] Noeske, et al. MRM 2000; 44: 978-82.

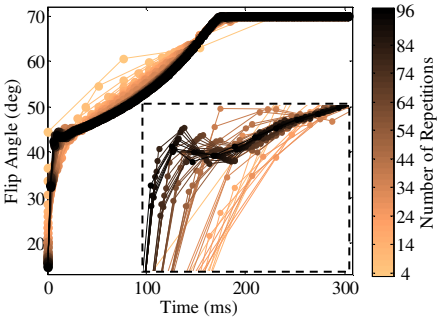

Fig. 1: Convergence of the variable flip angle schedule for the maximum myocardial SNR case (Myo: SNR). Successive iterations with more, shorter TR intervals have darker colors. Inset: the region near 15 ms.

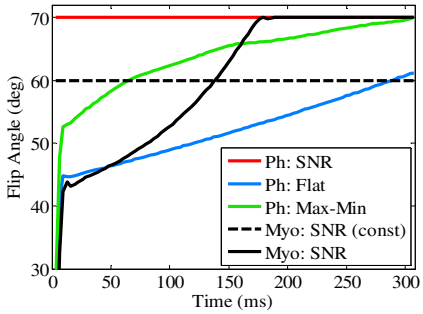

Fig. 2: Flip angle schedules for the phantom (Ph) and the myocardium (Myo). Schedules constrained to a constant angle are indicated (const).

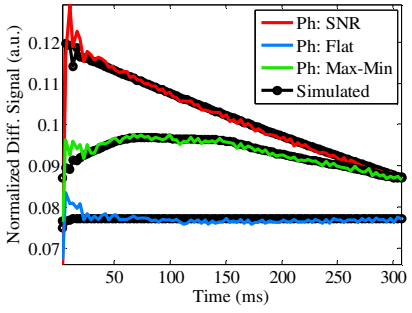

Fig. 3: Measured (colored) and simulated (black) difference signal profiles for the three optimized phantom schedules. The mean simulation error in each was < 0.5%.

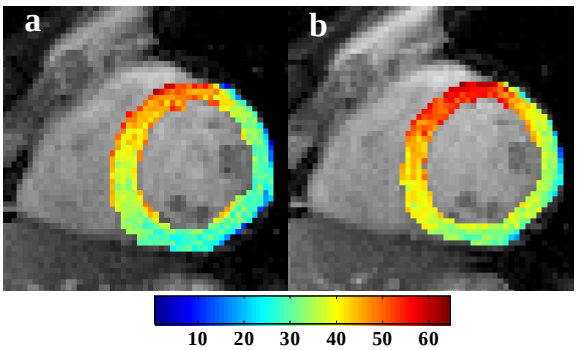

Fig. 4: Short axis difference images from max. myocardial SNR schedules using: (a) a constant flip angle and (b) variable flip angles. Myocardium pixels appear in color.